CLASSICAL AND QUANTUM CHAOS IN ROBERTSON-WALKER COSMOLOGIES

Roman Tomaschitz

Physics Department, University of the Witwatersrand,
Johannesburg, WITS 2050, South Africa

Abstract. An elementary review of my work on the physical impact of the topological structure of space-time is given. An account on classical chaos in an open, multiply connected universe is presented. The uniformity of the galactic background is related to the erratic behavior of the classical world lines around the chaotic nucleus of the universe. On the quantum level we discuss particle creation, backscattering, anisotropy in the microwave background, parity violation and how all this relates to the multiple connectivity of the open spacelike slices.

1. INTRODUCTION

If one agrees to do cosmology on the basis of a space-time continuum, a Riemannian four-manifold, one is soon confronted with the choice of the topology. What is the global topological structure of space-time? This question was immediately raised by the mathematician Felix Klein, when Einstein proposed his first cosmological model, but it was not until much later, that the topological impact on geodesic motion gained serious consideration [1, 2].

Is the universe finite or infinite? Most laymen, and I think also philosophers, would attach to the word "Universe " the attribute "infinite". Many physicists however believe that finite models of the universe are handier for heuristic reasoning. In fact, the idea that the physical universe is infinite was rejected by Jordan on the grounds that we will never be able to look at infinity and verify what is happening there [3]. What he overlooks is that the global structure can manifest itself in (microscopic) physical phenomena.

Deterministic Chaos in General Relativity
Edited by D. Hobill *et al.*, Plenum Press, New York, 1994

We will see, cf. Sec. 3, that an infinite and multiply connected universe has a chaotic center [4, 5], that may well account for the equidistribution of the galaxies. Some kind of chaos is in my opinion necessary to achieve this, the actual problem here is not only to explain the uniformity, but rather the apparent deviations from perfect homogeneity.

The crucial question is not so much what *is* the topological structure of the universe, but rather *how does it evolve*. An infinite universe has indeed the ability to evolve [6], contrary to closed ones, whose time evolution is confined to a trivial rescaling of the length unit on the spacelike slices. In Sec. 5 we will discuss this evolution in terms of global metrical deformations of the spacelike slices, global in the sense that the local curvature stays constant. We show how simple coordinate transformations in the covering space can generate such deformations, and how they distort the center of the 3-slices. In Sec. 6 we show how this evolution provides a dynamical mechanism for particle creation [6, 7]. In Sec. 7 we demonstrate how such deformations generate an angular dependence in the temperature of the microwave background [7, 8]. In Sec. 8 we sketch how the topology of the universe leads to the non-conservation of parity [9], and to a possible explanation of the baryon asymmetry. Finally I mention here the fascinating possibility of a multiple connectivity of space-time in the small [10], and of particles emerging as topological excitations.

In Secs. 2 and 3 we give an introductory and more or less self-contained account on the geodesic problem in open hyperbolic 3-manifolds [11-14]. In Sec. 4 we discuss how this relates to chaos in RW-cosmologies[4, 5]. The quantum mechanical ground state problem for chaotic wave fields localized on the center of the 3-slices [4, 15], the dispersion phenomenon in RW-cosmologies, and horospherical flows [7,16] are reviewed in [17].

2. SOME ELEMENTARY GEOMETRICAL AND TOPOLOGICAL CONCEPTS

In this Section we sketch some methods to study the global behavior of geodesics on a 3-manifold in a quantitative way. With geodesic we mean here the shortest path between two points compared to all neighboring paths. The emphasis lies here on "neighboring", because in a multiply connected space the geodesic variational problem has several local minima, if the two points lie sufficiently far apart. With geodesics we mean such local minima.

Global variational problems are in practice much harder to solve than local ones. In the case of multiply connected manifolds, the universal covering space construction provides a very efficient way to do that. The geodesics as we discuss here turn out to be the spacelike projections of the world lines in the RW-cosmologies discussed in Sec. 4. Let us start with an example.

The simplest example of a multiply connected hyperbolic 3-manifold is a solid torus, topologically the product of a finite interval and an annulus. It is best modeled in the Poincaré half-space H^3, its universal covering space: the complex plane with a t-axis perpendicular to it, $t > 0$ (t denotes always a space coordinate), and a line element $d\sigma^2 = t^{-2}(|dz|^2 + dt^2)$. In this way we get an isometric copy of the Minkowski hyperboloid, i.e. hyperbolic space H^3. The geodesics are either straight lines perpendicular to the complex plane or semicircles orthogonal to it. The totally geodesic planes are therefore either hemispheres on $\mathbb{C}$ or Euclidean half-planes perpendicular to $\mathbb{C}$ [12].

To construct the torus we place two concentric hemispheres with radii $r = 1$ and $r = |\alpha| > 1$, $\alpha \in \mathbb{C}$, onto the complex plane, see Fig. 1a, and identify them by the transformation $T_\alpha(z,t) = (\alpha z, |\alpha| t)$. This T_α leaves the metric on H^3 invariant. If α is positive the identification happens radially, if it is complex we rotate the hemispheres against each other before we identify them. The hyperbolic polyhedron F bounded by the two hemispheres and the annulus between their base circles in the complex plane is topologically a solid torus if we perform the above identification with T_α, see Figs. 1a,b. The metric $d\sigma^2$ of H^3 gets induced onto F, and (F, T_α) is thus a hyperbolic manifold.

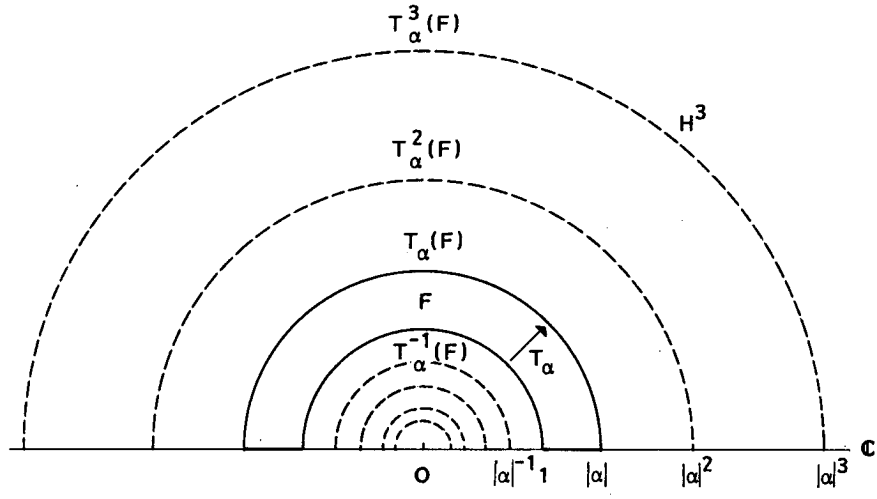

Figure 1a. Section through the Poincaré half-space H^3 .We place two concentric hemispheres of radii 1 and $|\alpha|$ onto the complex plane. F is the polyhedron bounded by these two hemispheres and the annulus between the base circles in $\mathbb{C}$. If we identify the two hemispheres radially (indicated by the map T_α), then (F, Γ) is topologically a solid torus, cf. Fig. 1b. The covering group Γ consists of all integer powers T_α^n. The images $T_\alpha^n(F)$ provide a tiling of H^3, as well as of $\mathbb{C}$, the boundary at infinity of H^3 , with concentric hemispherical shells and annuli respectively. The tiles have two accumulation points in $\mathbb{C}$, namely 0 and ∞. $\Lambda(\Gamma)$ is the limit set of Γ.

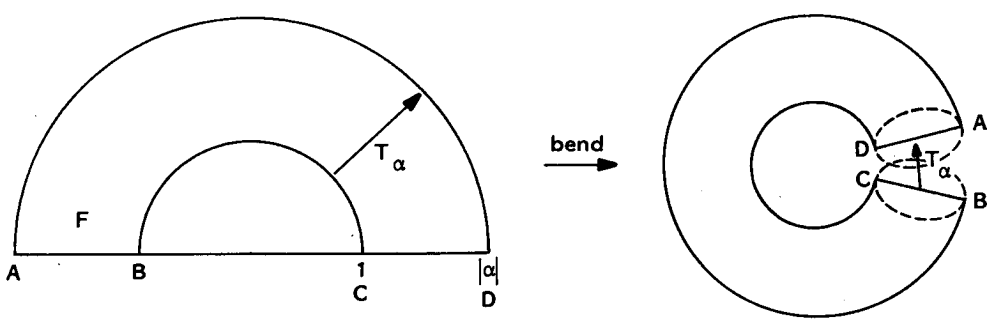

Figure 1b. If the polyhedron F is bent in the indicated way, it is quite obvious that (F, Γ) gives topologically a solid torus. Its boundary is the 2-torus obtained by identifying the boundary circles of the annulus in the complex plane. The hyperbolic metric gets singular at $\mathbb{C}$. Therefore (F, Γ) is an open 3-manifold.

One can now pose the question how many hyperbolic (i.e. of curvature -1) 3-manifolds with the topology of an open solid torus (the product of a finite open interval with an annulus) do exist. Sufficiently small coordinate patches on two hyperbolic manifolds can always be mapped isometrically onto each other, because they have the same curvature. Here however we must ask if there exists a global isometry, a diffeomorphism of a solid torus onto another, that respects the metric. The answer is that different α (in T_α) correspond to different, globally non-isometric (non-isotopic) solid tori.

In order that (F, T_α) is a Riemannian manifold, the induced metric has to fit smoothly on the identified hemispheres. There is a simple criterion for that. We define Γ, the covering group, as the set of all integer powers of T_α . Then the images $T_\alpha^n(F)$ of the polyhedron F under Γ must give a tiling of the covering space H^3. This tiling is depicted in Fig. 1a. The tiles have two accumulation points, 0 and ∞, the limit set $\Lambda(\Gamma)$. These accumulation points at infinity play an important part in analyzing the global behavior of geodesics, as well as in the spectral analysis of wave equations on the manifold [4, 8, 9].

By means of the covering group Γ and the polyhedral tiling $\Gamma(F)$ of H^3 we can project geodesics of the covering space H^3 into the 3-manifold (F, Γ). Consider a geodesic s (semicircle orthogonal to the complex plane) in H^3. It intersects a finite or infinite number N of polyhedral images, say $T_\alpha^{n_1}(F), ..., T_\alpha^{n_N}(F)$. Evidently we can label them as adjacent. We denote the arc of s lying in $T_\alpha^{n_i}(F)$ by s_{n_i}. So we can regard s as the ordered sequence of arcs $\{s_{n_i}\}_{i=1,...,N}$. The projection of s into (F, Γ) we define as the ordered sequence $\{T_\alpha^{-n_i}(s_{n_i})\}_{i=1,...,N}$ of arcs in F, cf. Sec. 8. Initial and end points of adjacent arcs, lying on the concentric hemispheres bounding F, are identified by T_α, so that we obtain a smooth geodesic in the 3-manifold (F, Γ). Every geodesic can be realized in this way. The whole works because the covering group Γ leaves the metric of H^3 invariant. We get so a perfectly quantitative realization of geodesic motion in the 3-manifold. The qualitative behavior of a geodesic depends very much on whether the initial and end points of the covering geodesic s are in the limit set $\Lambda(\Gamma)$, see Figs. 2-4.

3. THE CHAOTIC CENTER OF AN INFINITE, MULTIPLY CONNECTED 3-MANIFOLD

There are two generic classes of open hyperbolic 3-manifolds, namely solid handlebodies of genus $g \geq 1$ (the product of a finite open interval and a disc with some smaller discs removed), and thickened Riemann surfaces of genus $g \geq 2$, (the product of a finite open interval and a sphere with g handles attached). All that what has been said about the solid torus in Sec. 2 carries easily over to these cases [13, 14], and so we sketch them very shortly here.

The covering space constructions are indicated in Figs. 5-7, to which we refer in the following. The 3-manifolds (F, Γ) are again represented by a polyhedron F whose faces are identified in pairs by transformations T_i that leave the H^3- metric invariant. The covering group Γ is now the discrete group consisting of all words with letters $T_i^{\pm 1}$. If we apply Γ to F we get a tiling of H^3, which means that the Γ-images of F (apart from the identity) fill the interior of the hemispheres that bound F, cf. Figs. 5a and 6a. These images have accumulation points in the complex plane, like 0 and ∞ in Fig. 1a. In the case of Fig. 5 they constitute a Cantor set $\Lambda(\Gamma)$, totally disconnected and dense in itself, but not self-similar [18], in Fig. 6a they are a closed, fractal curve. The

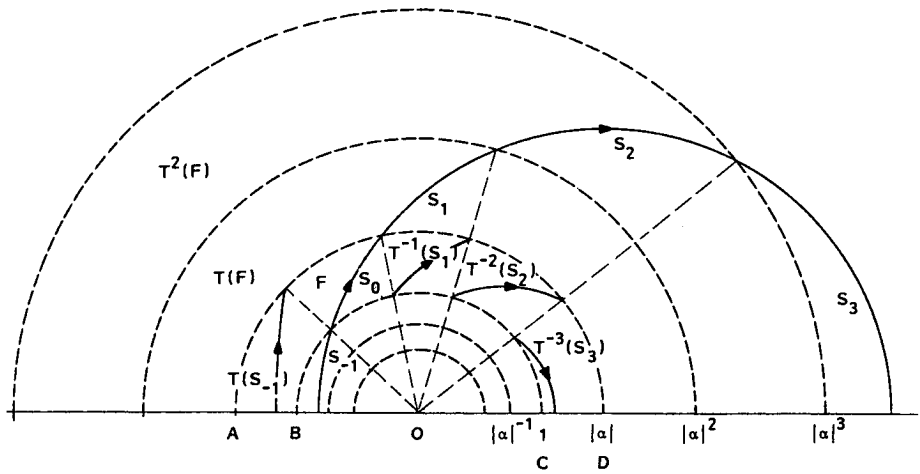

Figure 2a. The covering space construction, namely the representation of a 3-manifold as a polyhedron F with face-identification, is the appropriate means to study quantitatively geodesic motion on a multiply connected manifold. Every trajectory in (F, Γ) can be obtained by projecting a covering trajectory (semicircle in H^3) into the polyhedron F. The arc s_n, lying in the tile $T_\alpha^n(F)$, is mapped into F by $T_\alpha^{-n}(F)$. The trajectory in the 3-manifold appears now as the ordered sequence of arcs $(T_\alpha(s_{-1}), s_0, T_\alpha^{-1}(s_1), T_\alpha^{-2}(s_2), T_\alpha^{-3}(s_3))$. The initial and end points of the arcs are identified by T_α, as indicated by the hatched rays.

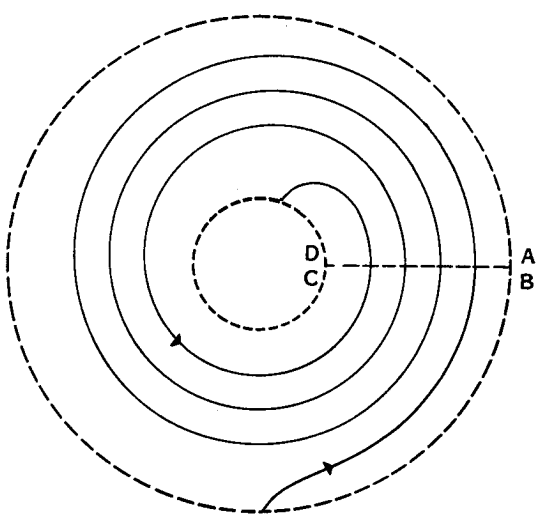

Figure 2b. The topology of the trajectory in Fig. 2a.

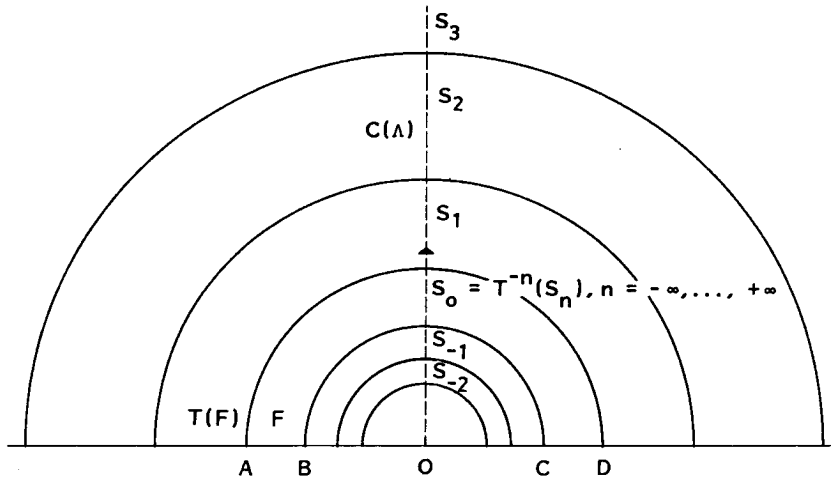

Figure 3. The covering trajectory is here a straight line $(s_{-\infty}, ..., s_0, ..., s_\infty)$, connecting the two limit points 0 and ∞. Its projection into F is s_0, infinitely covered by the images $T_\alpha^{-n}(s_n)$. s_0 is the only closed geodesic loop. It introduces a length scale in this infinite space. The hyperbolic length of this loop is $\log|\alpha|$.

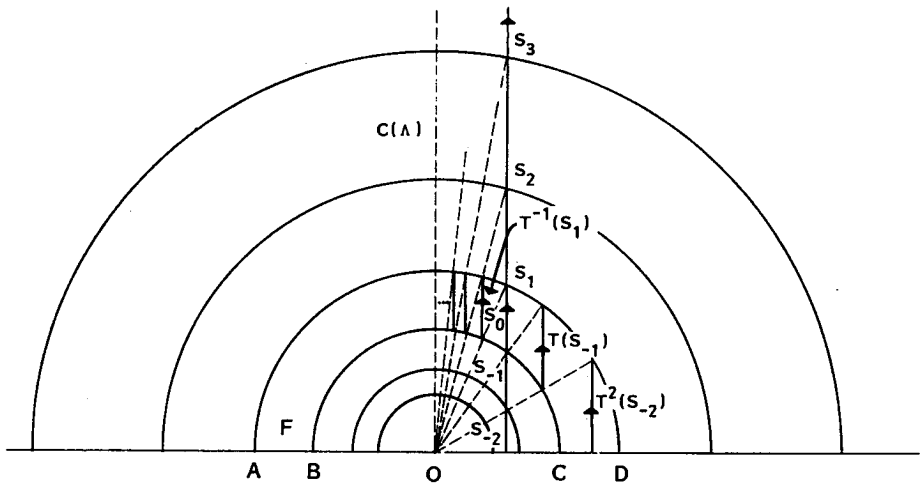

Figure 4a. The covering trajectory $(s_{-2}, ..., s_0, ..., s_\infty)$ has only one end point, ∞, in the limit set. The projected arc pieces $T_\alpha^{-n}(s_n)$ accumulate at the limit cycle, cf. Fig. 3.

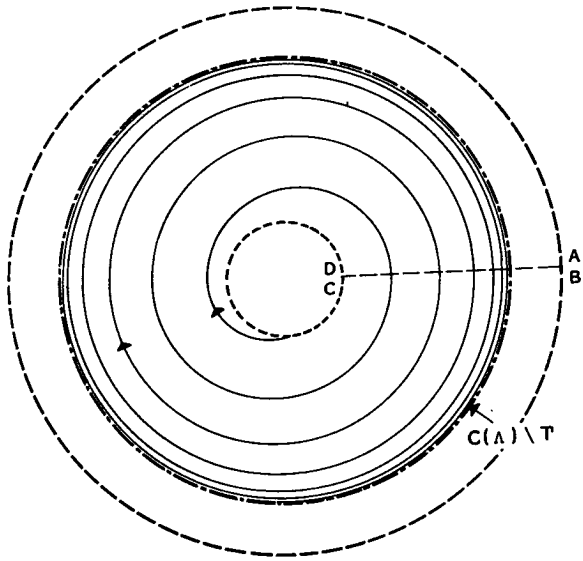

Figure 4b. The topology of the trajectory in Fig. 4a. Starting at infinity, it loops asymptotically into the limit cycle.

tiling $\Gamma(F)$ of H^3 induces a tiling of the complex plane, which can be used to determine the limit set $\Lambda(\Gamma)$, cf. Figs. 6b and 7a-c.

Geodesic motion on these multiply connected manifolds (F, Γ) can be realized in the same way as in the case of a solid torus, cf. Figs. 1-4, by projecting a H^3-geodesic with the covering group Γ into F.

Let us look on the qualitative behavior of trajectories, keeping in mind Figs. 1-4. What is the analogue to the closed geodesic loop in Fig. 3? Let us start with the 3-manifold that has as limit set $\Lambda(\Gamma)$ a circle, cf. Fig. 6b. Consider the set of all the covering geodesics that have initial and end points on this circle. These arcs cover the hemisphere $C(\Lambda)$ placed on the circle. This hemisphere intersects all the polyhedral faces erected on the base circles in Fig. 6a. Consider the region of this hemisphere that lies above the polyhedral faces. We identify its boundary arcs, which lie on the polyhedral faces, as indicated in Fig. 6a. In this way we obtain a closed surface of genus two, a doughnut. This Riemann surface embedded in the 3-manifold is the analogue to the closed loop of Fig. 3. Clearly this surface has finite area, a metric of constant curvature -1 is induced on it from H^3: it is the center $C(\Lambda) \setminus \Gamma$ of the open 3-manifold (F, Γ).

Bounded geodesics in (F, Γ) have covering geodesics which have initial and end points in the limit set (as is the case in Fig. 3). It is easy to see that all these bounded geodesics lie in the center $C(\Lambda) \setminus \Gamma$. Geodesics on such a compact surface have all kinds of chaotic properties, almost all are densely filling the surface, some are closed loops.

We ask what happens with a trajectory that has a covering trajectory whose initial and end points are not in $\Lambda(\Gamma)$, but very close to it. The corresponding geodesic in the 3-manifold will still tend from infinity to infinity, as in Fig. 2, but it will loop a long time in a region close to the center. Such geodesics are not dense or ergodic or mixing or whatever in the strict mathematical sense, but in any practical way they will appear as such, provided that the end points of the covering geodesic are close enough to the limit set. This is important, for in my opinion some kind of erratic

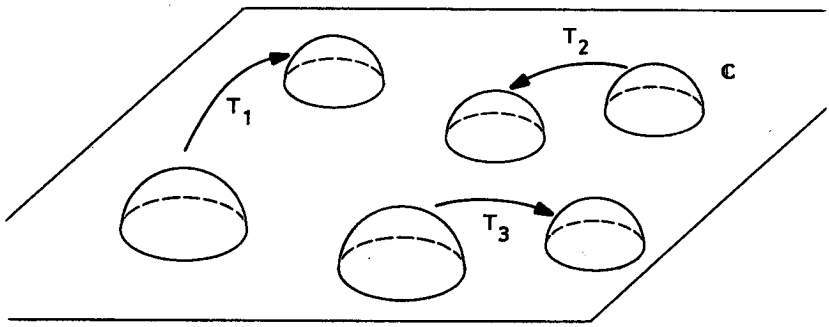

Figure 5a. Covering space construction of a handlebody. We choose $2g$ mutually disjoined hemispheres and identify them in pairs with elements T_i of the invariance group of the hyperbolic metric, so that T_i maps the outside of one sphere onto the interior of the other. The polyhedron F is now the space above the hemispheres and the complex plane. The polyhedral faces are the hemispheres, and there is one face at infinity of H^3 , analogous to the annulus in Fig. 1, namely the compactified complex plane with the $2g$ discs under the hemispheres removed.

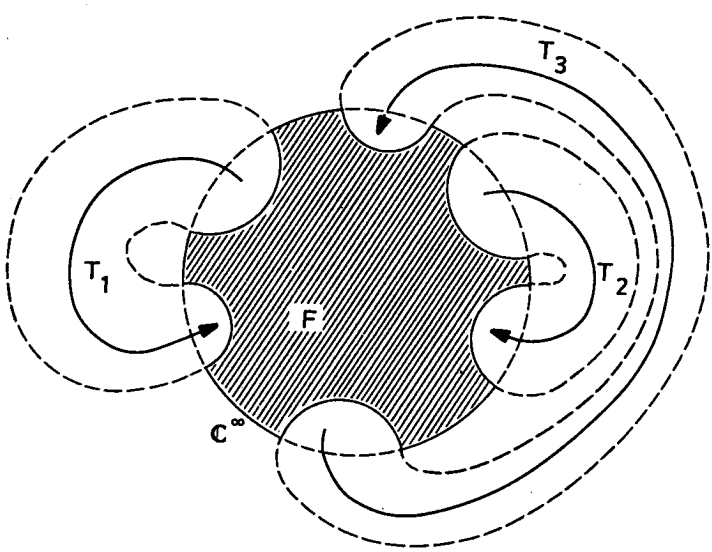

Figure 5b. The topology of the 3-manifold (F, Γ) in Fig. 5a. We compactify H^3 to a ball. Its boundary at infinity is the Riemann sphere. The polyhedron F is the hatched region. We identify the spherical caps as indicated. Topologically we attach in this way three solid handles to the ball.

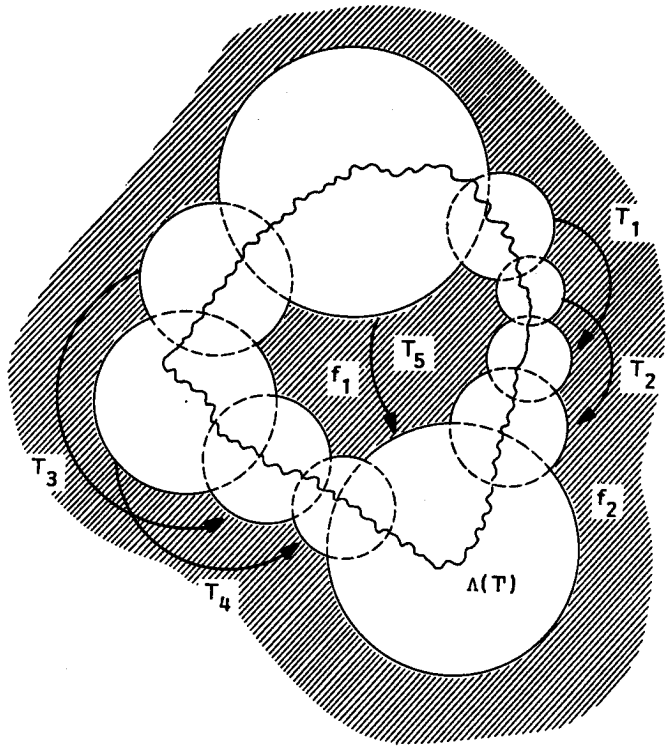

Figure 6a. Covering space construction for a thickened Riemann surface of genus two. Indicated are the base- circles of the hemispheres in the complex plane. Three-manifolds of this type can be realized by a ring of intersecting hemispheres with a suitable identification (T_i). The polyhedron F comprises the space above the hemispheres and the two faces f_1 and f_2 (hatched) at infinity. There is an analogue to Fig. 5b.

geodesic behaviour is necessary to account for the more or less uniform distribution of the galaxies. This uniformity does not seem to be perfect at all, and what is provided here is just a mechanism of imperfect classical chaos to achieve that.

The example in Fig. 6b is not yet generic for an infinite hyperbolic 3-manifold. Such a manifold has a limit set of non-integer Hausdorff dimension, cf. Figs. 7a-c. In this case the center of the 3-manifold is a three-dimensional finite domain: we start with the collection of all semicircles orthogonal to the complex plane which have their initial and end points in the fractal curve, and construct the hyperbolic convex hull $C(\Lambda)$ of them. This is now a three- dimensional domain. We consider the part of this domain that lies above the hemispheres in Fig. 6a, and identify its boundaries as indicated. We obtain a three-dimensional finite domain in the 3-manifold, which is itself not a manifold because it is pleated [13] due to the fractal nature of the limit set. The scenario concerning geodesic motion is otherwise quite similar to the foregoing. The bounded chaotic trajectories lie in this center, and nearly chaotic trajectories loop close to it.

4. GEODESIC MOTION IN MULTIPLY CONNECTED RW-COSMOLOGIES

These cosmologies are topologically the product of a hyperbolic 3-manifold and a time axis, $R^{(+)} \times (F, \Gamma)$, the time axis $R^{(+)}$ may be infinite, semi-infinite or whatever. The line element in the covering space $R^{(+)} \times H^3$ is $ds^2 = -c^2 d\tau^2 + a^2(\tau) d\sigma^2$, with $d\sigma$ as in Sec. 2. The corresponding metric we denote by $g^{RW}_{\mu\nu}$, the a^2-scaled Poincaré metric on

Fig. 6b

the spacelike sections we denote in the following by g^P_{ij}. The metric $g^{RW}_{\mu\nu}$ gets induced on $R^{(+)} \times (F, \Gamma)$. Solving the geodesic equations in $R^{(+)} \times H^3$, we realize that the spacelike projections of the world lines are the covering geodesics described in Secs. 2 and 3. Their projections into (F, Γ) inherit the time parametrization of the covering trajectories. A covering trajectory will not reach the boundary at infinity of H^3 within a finite time. That means that its projection into the center of the 3-slices can be dense at best in the limits $\tau \to 0, (-\infty), +\infty$, i. e. backwards in time or at the end of the expansion. It may also happen, depending on the expansion factor a, that the covering trajectory does not reach the boundary even in these limits. That means that the actual covering trajectory is only a finite arc, well separated from the complex plane. If we project this arc into the center $C(\Lambda) \setminus \Gamma$, we get a trajectory of finite length. This trajectory may come close to every point in the center, but it is not dense in the strict sense.

Summing up, there is a large proportion of trajectories, namely those whose covering geodesics have end points close to the limit set (this set can have a dimension close to two), which will spend a long time in a domain close to the center of the 3-manifold, looping around there in an erratic way. This can be a mechanism to generate the current imperfect uniformity of the galactic background [6, 8].

Concerning Einstein's equations in this context [19], we mention that the curvature tensor of the covering space projects as it stands onto $R^{(+)} \times (F, \Gamma)$, likewise the energy-momentum tensor. This is so because their dependence on the space coordinates is only via the Poincaré metric, and thus both tensors are invariant with respect to the covering group. There is always the same well known relation between pressure, density, and the expansion factor, independent of the topology. Therefore it seems to me difficult to gain information about the evolution of the universe on a global level by means of Einstein's equations. In my view it is also a mistake to rely on the positivity arguments for pressure

Figure 6b. A tiling on the boundary of H^3 that is induced by the tiling $\Gamma(\mathbf{F})$. The domain in the middle is the hatched domain f_1 in Fig. 6a, bounded by circular arcs on the base circles. The accumulation points of the tiles define in this case a circle $\Lambda(\Gamma)$, corresponding to the closed curve indicated in Fig. 6a. All tiles are Γ-images of f_1.

Fig. 7a-c

Fig. 7a

Fig. 7b

Fig. 7c

Figure 7a-c. Different realizations of the pattern of base circles give rise to globally non-isometric manifolds. Depicted is a sequence of deformations of the polyhedron F in Fig. 6b. To obtain the polyhedral tiling of H^3 we extend the circular arcs that bound the tiles to circles, and place hemispheres onto them. The fractal boundary curves of the depicted tilings are continuous images of the limit circle in Fig. 6b. They have a Hausdorff dimension $1 < \delta < 2$, but they are not self-similar. These fractal limit sets at the boundary of the covering space determine the qualitative properties of geodesics in the 3-manifold.

and energy derived from them, which make statements about the asymptotic form of the expansion factor. The predictions derived in this way are fairly unacceptable, despite of attempts to rescue them by means of information theoretical and biological arguments [20]. Dyson claims that time is without end, which naturally raises the question if time is also without beginning...

5. EXTENDED RW-COSMOLOGIES

All that what has been said so far refers to a static 3-space geometry, the spacelike slices (F, Γ) are time independent, and so is the RW-metric in the covering space, apart from the trivial time-dependence via the expansion factor. However, the polyhedron F together with its face-identifying transformations T_i can vary. For example, the α in Fig. 2 may describe some path in the region $|\alpha| > 1$. Different α correspond to globally non-isometric 3-manifolds of curvature -1, cf. Sec. 2. There is another way to describe this variation of the 3-manifold in its deformation space, the region $|\alpha| > 1$. We keep the polyhedron F as well as the covering group time independent, which is necessary if we want to attach to the 3-manifold a time axis, and vary instead the Poincaré metric g^P_{ij} in H^3, which is induced onto (F, Γ). To vary means here that we replace it by a time dependent tensor field $\tilde{g}_{ij}$, which is periodic, i.e. invariant, with respect to the covering group Γ. Instead of ds^2 we consider $d\tilde{s}^2 = -c^2 d\tau^2 + \tilde{g}_{ij} dx^i dx^j$, $x^i = (x, t)$, on $R^{(+)} \times (F, \Gamma)$. The covering geodesics are now more complicated curves, but the projection mechanism into the 3-manifold remains unchanged.

Let us discuss that a little more explicitly. Imagine that there are two tori, as in Sec. 2, (F, T_α), $\alpha > 1$, and (F_λ, T_λ), $T_\lambda : (z, t) \to \alpha^\lambda(z, t), \lambda > 0$, with F_λ the polyhedron defined by the hemispheres $r = 1$ and $r = \alpha^\lambda$. We construct a diffeomorphism h of H^3, so that $hT_\alpha h^{-1} = T_\lambda$. We have $h : (x, y, t) \to (x^2 + y^2 + t^2)^{(\lambda-1)/2}(x, y, t), (x, y, t) := x^i$. If we apply the coordinate transformation h to g^P_{ij} we obtain

$$\tilde{g}_{ij} = a^2(\tau) t^{-2} (\delta_{ij} + (\lambda^2 - 1)(x^2 + y^2 + t^2)^{-1} x^i x^j)$$

This metric is still invariant with respect to the discrete group generated by T_α. If we impose $\tilde{g}_{ij}$ onto the polyhedron F, we get a hyperbolic 3-manifold $(F, T_\alpha, \tilde{g}_{ij})$ which is isometric to (F_λ, T_λ). This means that we can represent (F_λ, T_λ) by the same covering group and the same polyhedron as the manifold (F, T_α), provided we replace g^P_{ij} by $\tilde{g}_{ij}$. Note that the length of the limit cycle of (F_λ, T_λ) is $\lambda \log \alpha$, cf. the caption of Fig. 3. We denote by $\tilde{H}^3$ the upper half-space endowed with $\tilde{g}_{ij}$. The 3-manifold represented as $(F, T_\alpha, \tilde{g}_{ij})$ with covering space $\tilde{H}^3$ we can then easily extend to a 4-manifold using the line element $d\tilde{s}^2$ as indicated above. The crucial point here is that this extension remains possible even for a time-dependent λ. In this case we cannot use (F_λ, T_λ) , $g^{RW}_{\mu\nu}$ (cf. Sec. 4), and $R^{(+)} \times H^3$, because $g^{RW}_{\mu\nu}$ is not invariant with respect to the time-dependent covering group generated by $T_{\lambda(\tau)}$. As pointed out in Sec. 2, $\lambda(\tau)$ describes a path in the deformation space of the topological manifold. The spacelike slices have always curvature $-1/a^2(\tau)$, independent of $\lambda(\tau)$. The energy momentum tensor, defined by the Einstein tensor and $d\tilde{s}^2$ in $R^{(+)} \times \tilde{H}^3$ projects onto the manifold $R^{(+)} \times (F, T_\alpha, \tilde{g}_{ij})$.

Concerning the technical problem of calculating geodesics and wave fields in the covering space $R^{(+)} \times \tilde{H}^3$ endowed with $d\tilde{s}^2$, we assume that $\lambda(\tau)$ is varying adiabatically. Then $d\tilde{s}^2$ is approximately generated by applying the transformation

$\tau \to \tau, x^i \to h^i(x,\tau)$, to the RW-line element ds^2, cf. Sec. 4. The $g_{0\mu}$, which make the difference, can be taken into account by Green-Liouville asymptotics. If h^i is independent of time this correspondence between ds^2 and $d\tilde{s}^2$ is exact, and shows how a coordinate transformation in the covering space can give rise to non-isometric manifolds. Infinitesimal gauge transformations are generated by vector fields that are invariant with respect to the covering group, which is clearly not the case with the transformation h^i.

If we consider generic 3-manifolds with non-abelian covering groups, cf. Sec. 3, we have to construct a diffeomorphism h of H^3, so that the hT_ih^{-1} are again Möbius transformations. This is rather tedious to do in practice, see [5] for a similar problem in two dimensions, and there is a simpler way to realize small global deformations, without explicit knowledge of h.

We construct $\tilde{g}_{ij}$ by adding to the Poincaré metric a field h^Γ_{ij} that is invariant with respect to the covering group Γ, $\tilde{g}_{ij} = a^2(\tau)(t^{-2}\delta_{ij} + h^\Gamma_{ij})$. Such invariant tensor fields can be generated by periodizing an arbitrary symmetric field $h_{ij}(z,t,\tau)$ on H^3 :

$$h^\Gamma_{ij}(z,t,\tau) = \sum_{\gamma\in\Gamma} h_{kl}(\gamma(x,t),\tau)\,[\gamma'(z,t)]^k_i\,[\gamma'(z,t)]^l_j\,,$$

where γ' denotes the Jacobian of the Möbius transformation. Because $\tilde{g}_{ij}$ is invariant with respect to Γ, $(F,\Gamma,\tilde{g}_{ij}(\tau))$ is a manifold with covering space $\tilde{H}^3$. Clearly, for arbitrary fields h_{ij} this manifold will not be of constant curvature. To insure that, the Ricci tensor must be proportional to $\tilde{g}_{ij}$. If h^Γ_{ij} is small we may linearize $R_{ij}(\tilde{g})$, using as background metric the Poincaré metric. The resulting equation for h^Γ_{ij} is invariant with respect to Γ. Therefore it is enough to find non-periodic solutions h_{ij} and periodize them as shown above, compare the spectral analysis of the electromagnetic field in this context [8].

Finally, I would like to comment on Euclidean cosmologies of finite size, cf. [21], which show a certain resemblance with Mixmaster models, and where it is particularly easy to construct the diffeomorphism h and the deformation space.

We consider the Minkowski line element on $R^{(+)} \times R^3$, and the Euclidean 3-manifold (F_c,Γ_c), namely the unit cube F_c in R^3, with opposite faces identified in pairs by Euclidean translations, the generators of Γ_c. Next we consider a parallelepiped $\hat{F}$ generated by the vectors $\vec{a} := (a,0,0)$, $\vec{b} := (b_1,b_2,0)$, $\vec{c} := (c_1,c_2,c_3)$; where a, b_i, c_i are real and opposite faces again identified by Euclidean translations, which generate a group $\hat{\Gamma}$. The Euclidean manifolds (F_c,Γ_c) and $(\hat{F},\hat{\Gamma})$ are isometric iff F_c and $\hat{F}$ are congruent. We construct readily a linear transformation h in R^3, that maps F_c onto $\hat{F}$, so that we have $h\Gamma_c h^{-1} = \hat{\Gamma}$. Evidently $(\hat{F},\hat{\Gamma})$ is isometric to $(F_c,\Gamma_c,\tilde{g}_{ij})$, $\tilde{g}_{ij} := \delta_{mn}h^m_{,i}h^n_{,j}$. The coefficients a, b_i, c_i are arbitrary functions of time. They parametrize completely the six-dimensional deformation space. If we replace δ_{ij} in the Minkowski metric by $\tilde{g}_{ij}$ we get the line element $d\tilde{s}^2$ of the covering space $R^{(+)} \times R^3$. If $b_1 = c_1 = c_2 = 0$, we have $\tilde{g}_{ij} = diag[a^2(\tau), b_2^2(\tau), c_3^2(\tau)]$ on the spacelike slices (F_c,Γ_c). The expansion factors appear here as a path in the deformation space.

6. TOPOLOGICAL BACKSCATTERING AND PARTICLE PRODUCTION IN ELECTROMAGNETIC AND NEUTRINO FIELDS.

In Secs. 2 and 5 we discussed how an open hyperbolic 3- manifold can undergo global metrical deformations, without changing its constant curvature. In fact this condition

can be relaxed, there is no necessity to choose a priori constant curvature, nearly constant curvature and a metric that is uniformly close to the Poincaré metric will likewise do. The covering space formalism is sufficiently flexible to incorporate also large local perturbations and singularities.

In simply connected RW-cosmologies it is known for a long time [22, 23] that variations of the expansion factor can lead to particle creation in quantum fields, and to backscattering in classical fields. I mention here, that one does not need a rapidly varying expansion factor to obtain this effect, linear expansion causes in a simply connected open RW-cosmology particle creation in a massive Dirac field [9].

These effects cannot happen in conformally coupled fields, like neutrinos and electromagnetic fields, because in the solutions of the corresponding wave equations the expansion factor scales out with a simple power law [1, 24]. But global metrical deformations of the 3-space manifold do create particles even in conformally coupled fields, Fig. 8 illustrates how this comes about. We divide the time axis τ for simplicity into

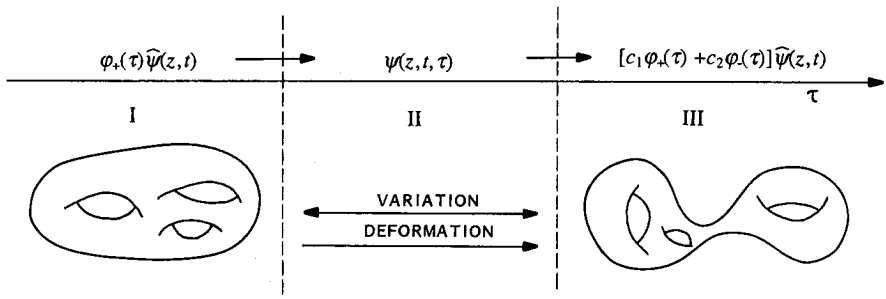

Figure 8. Global metrical deformations of the spacelike slices lead to particle creation and backscattering. A wave packet, initially composed of positive frequencies, receives an admixture of negative frequencies during the deformation.

three intervals. In I and III the metric ds^2 on the spacelike slices is time independent, apart perhaps from a time dependence via the expansion factor, that is irrelevant here. The polyhedron F as well as the covering group is time independent in all three intervals. Under these conditions the wave equation is time separable, and because the field is also conformally coupled, positive and negative frequencies can be unambiguously defined.

In the second interval a global metrical deformation takes place, the line element on the covering space is given now by $d\tilde{s}^2$ in Sec. 5. In this period the wave equation is not separable, and the particle/antiparticle concept loses its meaning here. Finally, in interval III, the general solution of the wave equation is a linear combination of positive and negative frequency modes. If the variation in II is generic, none of the coefficients c_1, c_2 will be zero. Therefore antiparticles are created in the quantum case, and a backscattered wave appears in the case of an electromagnetic field.

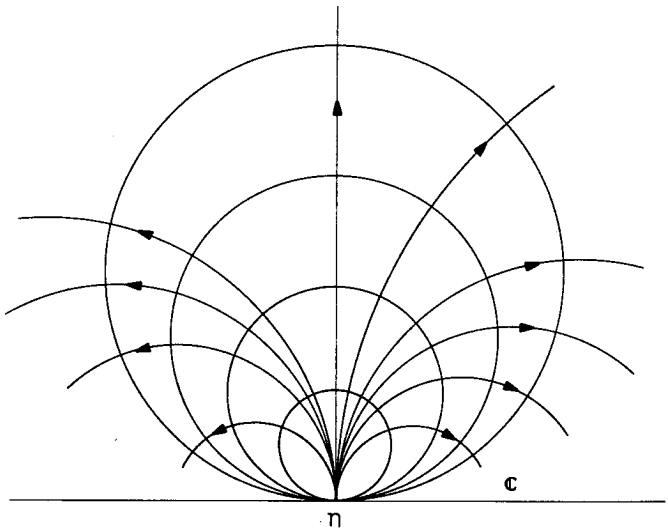

Figure 9. Wave fronts of horospherical elementary waves generated at a point η at infinity of H^3 (the horizon). They appear as the surfaces of constant phase in the eigenfunctions of the Maxwell equations. The bundle of rays issuing from η comprises their orthogonals. Accordingly the surfaces of constant action and phase coincide for rays and elementary waves emanating from a point at infinity.

7. ANGULAR FLUCTUATIONS IN THE TEMPERATURE OF THE MICROWAVE BACKGROUND

Angular anisotropy in the Planck distribution is a possible consequence of global metrical deformations of the spacelike slices. Let us start with a simply connected RW-cosmology and the line element ds^2 in Sec. 4. Because H^3 is homogeneous, it happens that the eikonal of geometric optics appears in the phase of the spectral elementary waves of the Maxwell equations in the covering space. This relation is in other systems only true approximately, semiclassically, here and in homogeneous spaces in general it is exact, cf. Fig. 9.

Geometric optics does not know the concept of momentum. However, we can attach to the rays a momentum via the Einstein relation $p_\mu = \hbar k_\mu$. So we obtain a vector field on H^3, $p_\mu(z,t,\tau;\eta,s)$, describing the momentum of a horospherical bundle of classical flow lines where s is a spectral parameter, labeling the elementary waves. The directions are labeled by η , cf. Fig. 9. It is easy to see that this flow, coming onto an observer at (z,t), is isotropic.

We project the horospherical bundles together with the vector fields attached to them into the 3-manifold (F,Γ). The spectral parameter η is now restricted to the region outside the base circles of the polyhedral faces, f_1 and f_2 in Fig. 6a, namely to the boundary at infinity of the 3-manifold. It is easy to see that for any given $p_\mu(z,t)$ in F there is exactly one ray coming from the boundary, that has this momentum at (z,t). Thus the flow stays isotropic, and we have again the same Planck distribution $\rho(h\nu/kT)$ as in Minkowski space.

Let us finally switch on adiabatically a global deformation $\tilde{g}_{ij}$ of the 3-space met-

ric, cf. Sec. 5, compare also [25] for the case of local fluctuations. The perturbed horospherical eikonal for rays issuing at some point η on the horizon, cf. Fig. 9, is $\tilde{\psi}^\Gamma = \psi^\Gamma + \chi(z,t,\tau,\eta)$, where χ is a periodic scalar field with respect to the covering group. The perturbed frequencies are $\tilde{\nu} = \nu\left(1 + \frac{1}{\omega}\frac{\partial\chi}{\partial\tau}\right)$, which means that we have to replace in $\rho(h\nu/kT)d\nu$ the temperature by $\tilde{T} = T\left(1 - \frac{1}{\omega}\frac{\partial\chi}{\partial\tau}\right)$, which amounts to an angular variation η of the temperature in the distribution, that remains otherwise unchanged [8]. The adiabatic time dependence of the temperature reminds us that we have here only a first approximation to a non-equilibrium process [26]. A further nice feature of these infinite cosmological models is that we can carry out the thermodynamic limit in them.

8. PARITY VIOLATION DUE TO SELF-INTERFERENCE OF SPACE-REFLECTED WAVES

A space reflection in the covering space H^3 is realized as $P(z,t) = (|z|^2 + t^2)^{-1}(-z,t)$. The center of this reflection is $(0,1)$; any other point in H^3 will likewise do, but the formula for P gets more complicated. The geometric meaning of $P(z,t)$ is that the point $(0,1)$ lies always in the middle of the geodesic joining (z,t) and $P(z,t)$.

The universal covering space construction provides here again an easy and explicit way to define a space reflection on the multiply connected 3-space [9]. At first we define the covering projection π^Γ, $H^3 \to F$, $\pi^\Gamma(z,t) = \gamma^{-1}(z,t)$, if $(z,t) \in \gamma(F)$. We refer here to the tiling of H^3 by images $\gamma(F)$, $\gamma \in \Gamma$, of the fundamental polyhedron F. The space reflection in (F,Γ) we define finally by $P^\Gamma(z,t) = \pi^\Gamma(P(z,t))$. The point of inversion is $\pi^\Gamma(0,1)$, which lies in the middle of a geodesic joining (z,t) and $P^\Gamma(z,t)$.

The classical geodesic equations are reflection invariant, but the situation is quite different concerning wave mechanics. Imagine a wave packet concentrated on a finite domain in the manifold (F,Γ). If we apply P^Γ, it can happen that the reflected wave wraps around a handle of the manifold, cf. Fig. 10. Note that the length of the geodesic loop in Fig. 3 can be arbitrarily close to zero. The wave packet starts to interfere with itself, and its norm is not preserved.

Because of this self-interference the space reflection symmetry is already broken on the level of the free Dirac equation. The T-symmetry is likewise broken because of the time dependence of the metric. C is still a good symmetry, but all combinations of C, P, and T are broken. That is remarkable, because usually one has to attach on purpose symmetry breaking interactions in order to achieve this. One can speculate if the baryon asymmetry can be topologically generated. Likewise, if one believes in topologically generated elementary particles, particles as topological/metrical excitations, one could try to understand CP violation as a self-interference effect.

9. CONCLUDING REMARKS

The ultimate aim of cosmology is perhaps to relate the microscopic laws of nature, that we describe now by Newtonian and quantum mechanics, to the global structure and the evolution of the universe. Examples for that are Mach's principle or Dirac's large number hypothesis.

The most important lesson that we have learnt from the revival of classical mechanics during the last two decades is that the instability and unpredictability of classical systems are more the rule than the exception, contrary to that what hitherto has been taught. Dispersion in low dimensional classical systems makes it in practice impossible to view Newton's equations as an initial value problem [5]. The global dynamics in the cosmology presented here is a good example for that. In fact, trajectories which loop a long time close to the chaotic center of the manifold are highly sensitive with respect to the initial data: if the covering trajectory is close to the limit set, then its projection into F consists of many arc pieces, and the initial error multiplies whenever two pieces are glued together.

This instability strongly suggests to use probability densities rather then world lines to describe the classical dynamics adequately. A formalism to do that my means of horospherical flows can be found in [7, 16]. One can then also use the fact that

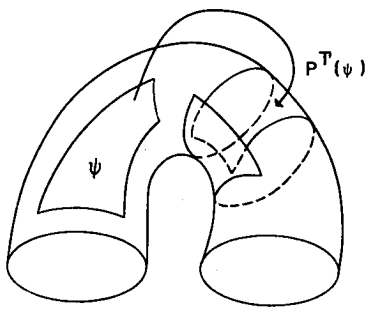

Figure 10. In two dimensions: a wave packet concentrated on a strip. The space reflection wraps the strip around the handle, so that it overlaps with itself. That results in self-interference.

the horospherical eikonal appears in the phase of the quantum mechanical elementary waves, to compare classical with quantum dispersion. Dispersion is inherent in the dynamics, whatever description one uses.

The phenomena reviewed here indicate that from the investigation of the topological structure of space and time further surprising consequences can be expected.

REFERENCES

[1] Infeld, L. and Schild, A., (1945), *Phys. Rev.*, **68**, 250.

[2] Schrödinger, E., (1956),*Expanding Universe*,, Camb. Univ. Press, Cambridge.

[3] Jordan, P., (1955), *Schwerkraft und Weltall*, 2nd ed., p. 113, Vieweg, Braunschweig.

[4] Tomaschitz, R., (1991), *J. Math. Phys.*, **32**, 2571.

[5] Tomaschitz, R., (1992), *Complex Systems*, **6**, 137.

[6] Tomaschitz, R., (1993), in *Proceedings of the XIX International Colloquium on Group Theoretical Methods in Physics*, (J. Mateos, ed.), CIEMAT, Madrid.

[7] Tomaschitz, R., (1993), *J. Math. Phys.*, **34**, 1022.

[8] Tomaschitz, R., (1993), *J. Math. Phys.*, **34**, 3133.

[9] Tomaschitz, R., (1993), "Cosmological CP violation", preprint.

[10] Wheeler, J. A., (1973), in *The Physicist's Conception of Nature*, (J. Mehra, ed.), D. Reidel, Dordrecht.

[11] Poincaré, H., (1985),*Papers on Fuchsian Functions* (J. Stillwell, ed.), Springer, New York.

[12] Fenchel, W., (1989), *Elementary Geometry in Hyperbolic Space*, de Gruyter, Berlin.

[13] Marden, A., (1980),*Bull. Am. Math. Soc. (New Series)* **3**, 1001.

[14] Maskit, B., (1986), *Kleinian Groups*, Springer, Berlin.

[15] Tomaschitz, R., (1992), in *Chaotic Dynamics: Theory and Practice*, (T. Bountis, ed.), Plenum, New York.

[16] Tomaschitz, R., (1994), to appear in *Intern. J. Theoret. Phys.*.

[17] Tomaschitz, R., (1994), in *Fractals in the Natural and Applied Sciences*, (M. Novak, ed.), to appear (Elsevier, Amsterdam).

[18] Akaza, T., (1964), *Nagoya Math. J.*, **24**, 43.

[19] Tomaschitz, R., (1992), in *Quantum Chaos-Quantum Measurement*, (P. Cvitanovic, ed.), Kluwer, Dordrecht.

[20] Dyson, F. J., (1979), *Rev. Mod. Phys.*, **51**, 447.

[21] Misner, C. W., Thorne, K. S. and Wheeler, J. A., (1973), *Gravitation*, Freeman, San Francisco.

[22] Schrödinger, E., (1939), *Physica*, **6**, 899.

[23] Birrell, N. D. and Davies, D. C. W., (1982), *Quantum Fields in Curved Space*, Camb. Univ. Press, Cambridge, UK.

[24] Parker, L., (1972), *Phys. Rev.*, **D5**, 2905.

[25] Sachs R. K. and Wolfe, A. M., (1967), *Astrophys. J.*, **147**, 73.

[26] Israel, W., (1972), in *General Relativity*, (L. O'Raifeartaigh, ed.), Clarendon Press, Oxford.